

# Robust Integrated Design for a Mechatronic Feed Drive System of Machine Tools

Chin-Yin Chen and Chi-Cheng Cheng

**Abstract**—This paper aims at to develop a robust optimization methodology for the mechatronic modules of machine tools by considering all important characteristics from all structural and control domains in one single process. The relationship between these two domains is strongly coupled. In order to reduce the disturbance caused by parameters in either one, the mechanical and controller design domains need to be integrated. Therefore, the concurrent integrated design method Design For Control (DFC), will be employed in this paper. In this connect, it is not only applied to achieve minimal power consumption but also enhance structural performance and system response at same time.

To investigate the method for integrated optimization, a mechatronic feed drive system of the machine tools is used as a design platform. Pro/Engineer and AnSys are first used to build the 3D model to analyze and design structure parameters such as elastic deformation, nature frequency and component size, based on their effects and sensitivities to the structure. In addition, the robust controller, based on Quantitative Feedback Theory (QFT), will be applied to determine proper control parameters for the controller. Therefore, overall physical properties of the machine tool will be obtained in the initial stage. Finally, the technology of design for control will be carried out to modify the structural and control parameters to achieve overall system performance. Hence, the corresponding productivity is expected to be greatly improved.

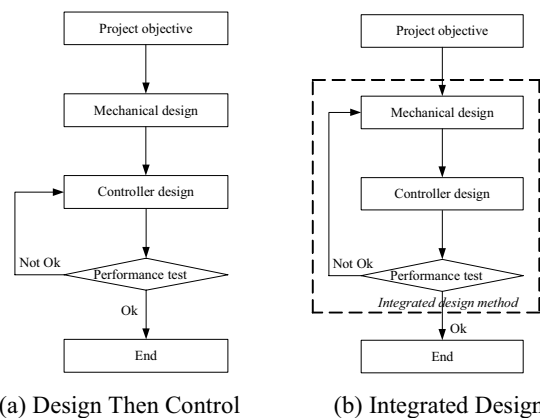
**Keywords**—machine tools; integrated structure and control design; design for control; multilevel decomposition; quantitative feedback theory

## I. INTRODUCTION

IN the recent past, machine tool manufacturers have introduced Numerical Control (NC) machine tools with high speed and high acceleration. Motion control and mechanism design issues in a feed drive system of NC machine tools therefore play an important role due to the demand of high speed machining. Additionally, the traditional method for developing mechatronic feed drive systems of machine tool is a kind of sequential strategy, which first optimizes the structure design then the control system [19, 20]. Such a sequential design and control strategy fails to achieve the true optimum because coupling exists between the design and control optimization problems. Consequently, the balance between

machinery and control needs to be addressed during the feed drive system design process.

The above mentioned traditional strategy for mechatronic design processes, which is usually referred to Design Then Control (DTC) approach, is shown in Fig. 1(a). In this strategy, the mechanical structure is usually designed first, and then fitted with off-the-shelf electric motors and drive electronics. Finally, a controller is designed and tuned for the existing physical system until the goal is achieved. Therefore, in this classical mechatronic system design process, the structural parameters are assumed to be fixed, and cannot be changed by excluding considerations for either whole system dynamics or control effort points of view. Consequently, this approach leads to a system with non-optimal dynamic performance. In view of the above reason, the recursive integrated design process, called Iterative Design (ID), as shown in Fig. 1(b) was developed for mechatronic systems. This recursive integrated design concept has been used in aviation, precision machinery, robotic, and hard disk designs.



(a) Design Then Control

(b) Integrated Design

Fig. 1 Classical design processes for mechatronic systems.

In the field of aviation, in 1985, Hale *et al.* [1], and Bodden and Junkins [2], separately proposed a rest-to-rest maneuver algorithm and an Eigenvalue optimization algorithm in view of the structure and controller design for flexible spacecrafts. In 1998, Messac [3] used a closed-form to accomplish the design task of a rotating structure.

Furthermore, in recent years, precision machinery has become widespread in almost all industrial fields. The mechanical and electrical domains of the mechatronic integrated design technology are constantly changing. In this field, Asada [4-5] focused on structure and controller design

C.-Y. Chen and C.-C. Cheng are with the Department of Mechanical and Electro-Mechanical Engineering, National Sun Yat-Sen University, Kaohsiung, Taiwan 80424, Republic of China (e-mail: d8932809@student.nsysu.edu.tw; phone: +886-7-525-4236; fax: +886-7-525-4299; e-mail: chengcc@mail.nsysu.edu.tw).

problems in 1990s. An optimization scheme with a recursive experiment analysis method was presented to tune the structure and controller parameters. Yang and Tu [6-7] used the multidisciplinary optimization and a parameter sensitivity method to solve the optimization problem in the structure and the controller design for hard disks in 1996. Recently, Fu and Mills [8] applied a convex optimal approach to design a linear motion system. In addition, as computer technology has gradually matured, some researchers concentrated on incorporating computer-aided design, modeling, and control schemes into the integrated design framework for mechatronic systems [9]-[11].

From those literatures, although the Eigenvalue method [1-2], the recursive method [4-5], the sensitivity function [6-7], and the convex optimal approach [8] were applied on mechatronic systems to obtain better system performance. However, they did not consider possible system's uncertainties during the system design process and regional structural design results were still used as the input of the controller design stage during the recursive process. This serial integrated design method leads to an increase of control costs and consequently, the whole system performance may not reach a satisfactory level.

Therefore, the goal of this paper is to develop a robust optimization methodology for the mechatronic modules of machine tools by treating all-important characteristics, from structural and control domains, as one single process. In this study, a mechatronic system of machine tools is broken into a two-level system including structure and control. In the first stage for the structural design process, a Pro/Engineer is used to build the 3D models and the AnSys is employed to design the mechanical structure and select the optimal components for the feed drive system. Next, in the control design process, a standard PID controller based on the Quantitative Feedback Theory (QFT) will be implemented to improve system robustness in the early design stage. Following this, three important parameters are established for the machine tool design to achieve overall system performance and reduce control cost.

The rest of this paper is organized as follows: the multilevel decomposition and the integrated design strategies will be formulated in section II. In section III, the presented mechatronic system design method will be employed in a feed drive system of typical machine tools, and an optimal QFT controller is implemented at same time. Finally, the conclusions will be drawn in section IV.

## II. INTEGRATED DESIGN STRATEGIES FOR A MECHATRONIC SYSTEM

With a multilevel decomposition approach [12], a large complex optimization problem is broken into a hierarchy of smaller optimization sub-problems and can be thought as levels of increasing details. At the upper level, the sub-problem is formulated in terms of global quantities, which describe the overall behavior of the entire system. On the lower level, the sub problems are stated in terms of local quantities and local constraints, which have only a small impact on the entire system. Each sub-problem uses local design variables to reduce

the violation of constraints, which are unique to that sub problem. Each level is a multi-objective optimization problem characterized by a vector of objective functions, constraints, and design variables. Therefore, considering the two-level structure and control problem for a mechatronic system, the multilevel decomposition procedure can be written as below.

At the structure level,

$$\begin{aligned} \min. \quad & Y_N(X_N), i=1, \dots, n_N \\ \text{s.t.} \quad & g_{Nk}(X_N) \leq 0, k=1, \dots, nc_N \\ & \sum_{i=1}^{NDV_N} \frac{\partial Y_{Rj}}{\partial X_{Ni}} \Delta X_{Ni} \leq \varepsilon_{2j}, j=1, \dots, n_R \\ & X_{Ni}^L \leq X_{Ni} \leq X_{Ni}^U, i=1, \dots, NDV_N \\ & X_{Rj}^L \leq X_{Rj}^* + \sum_{i=1}^{NDV_N} \frac{\partial X_{Rj}^*}{\partial X_{Ni}} \Delta X_{Ni} \leq X_{Rj}^U, j=1, \dots, NDV_R \end{aligned} \quad (1)$$

where  $Y_N$  and  $Y_R$  are the objective function vectors at the structure level and the control level, respectively;  $g_N$  is the corresponding constraint vectors;  $X_N$  and  $X_R$  are the corresponding design variable vectors,  $\varepsilon_{2j}$  is a tolerance on the change in the  $j^{\text{th}}$  objective of the control level during optimization at the structure level;  $L$  and  $U$  are lower and upper bounds of design vectors,  $\partial Y_{Rj}^*/\partial X_{Ni}$  and  $\partial X_{Rj}^*/\partial X_{Ni}$  represent the optimal sensitivity parameters of the control level objective function and design variable vectors, respectively, with respect to the structure level design variables.  $n_N$ ; and  $n_R$  denote numbers of objective functions for each level;  $nc_N$  is the number of constraints for the structure level;  $NDV_N$  and  $NDV_R$  individually denote design variables for the structure and control levels.

Similarly, the process of control level becomes

$$\begin{aligned} \min \quad & Y_R(X_N^*, X_R), j=1, \dots, n_R \\ \text{s.t.} \quad & g_{Rk}(X_N^*, X_R) \leq 0, k=1, \dots, nc_R \\ & X_{Ri}^L \leq X_{Ri} \leq X_{Ri}^U, i=1, \dots, NDV_R \end{aligned} \quad (2)$$

where  $X_N^*$  is the optimum design variable vector from the structure level and must be fixed during optimization at the control level.  $g_R$  denotes the corresponding constraint vectors

Following (1) and (2), the integrated design methodology can be classified into sequential designs, iterative designs (ID), and simultaneous design three strategies:

In the sequential strategy (also called DTC), the mechanical structure is usually designed first. Then, a controller is designed and tuned for the existing physical system until the goal is achieved (Fig. 1(a)). Therefore, the integrated design process of the DTC contains the following procedures:

1. Solve the optimal design problem according to (1).
2. Based on (2), solve the optimal controller problem to find corresponding optimal gains.

In this strategy, the structure is assumed to be fixed and cannot be changed by excluding considerations of whole system

dynamic point of view. Consequently, this approach brings about a system with a non-optimal dynamic performance. Hence, in order to improve the overall system performance, the ID strategy is appears.

For the ID strategy, the optimization procedure passes through the two levels before global convergence is achieved. A cycle is defined as one complete sweep through the two levels of optimization. In addition, optimization at an individual level requires several iterations before local convergence is obtained. Therefore, the steps for ID optimization design processes can be listed as below:

1. Solve the optimal design problem according (1).
2. Following (2), solve the optimal controller problem to find the corresponding optimal gains.
3. Return to steps 1 and 2, and satisfy the condition of (2a) until an optimal result is obtained. Where the suffix  $C$  is the number of time for optimization process.

$$Y_{Rc+1} \leq Y_{Rc} \quad (2a)$$

From the above description, it is assumed that, when the structure design variables  $X_N$  are fixed, all objective functions and constraints in the above design problem need to be convex. However it is not always true for the system level optimization problem to be convex [5]. Thus, in order to solve the optimization problem from the global system point of view, a simultaneous design strategy must be considered.

As (1) and (2), given an integrated structure and controller optimization problem for mechatronic systems, the system level is often non-convex, even if the individual structure and control optimization sub-problems are convex (individual design problems for (1) and (2)). The main reason involves static and variation optimization problems during the iterative design process. Thus, researchers have proposed the closed-loop Eigenvalues [2][3], Design For Control (DFC) [13], and convex integrated design [8] approaches to improve structure and control design performance simultaneous (Fig. 2).

In simultaneous design processes, the design objective of the system level is formulated as (2b), where  $\alpha$  and  $\beta$  are weighting factors, which adjust the corresponding relative importance of the structural objective function  $Y_N$  and the control objective function  $Y_R$ , and  $I_s$  is the global system performance index. Nevertheless, these two objective functions considered in the integrated design process interacts mutually and may have conflicting relationships. For example, minimization of the structural design error may contradict with minimization of the tracking error. As a result, for the integrated design of a mechatronic system, it is required to select proper design variables to achieve better results in terms of accuracy and response characteristics.

$$\min I_s = \alpha Y_N + \beta Y_R \quad (2b)$$

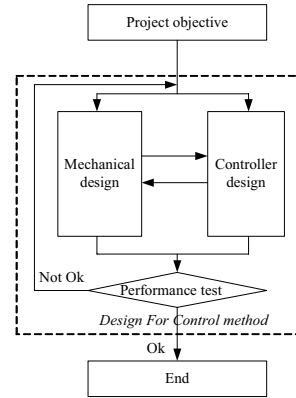


Fig. 2 Flowchart of Simultaneous design strategy

### III. DESIGN OF A MECHATRONIC FEED DRIVE SYSTEM

In this study, a classical feed drive system for machine tools as shown in Fig. 3 is considered. This system can be divided into three subsystems: mechanical structure, drive mechanism, and control unit. The system design specifications for this feed drive system are listed in Table I, where the position lose motion is defined as the position deviation caused by material deformation due to cutting force. The integrated design process of the feed drive system for machine tools will be presented in detail in this section.

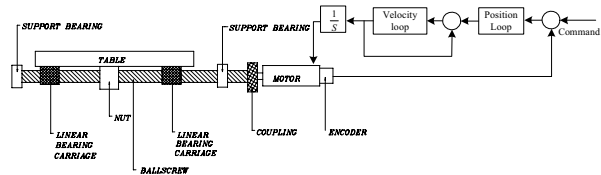


Fig. 3 Typical mechatronic feed drive system

TABLE I DESIGN SPECIFICATIONS

| Mechanical design parameters         | Specifications |
|--------------------------------------|----------------|
| Max speed of the table               | 40 m/min       |
| Max speed of the motor               | 2000 rpm       |
| Position accuracy                    | 2 $\mu$ m      |
| Micro-motion sensitivity             | 1 $\mu$ m      |
| Travel of the table                  | 400 mm         |
| Max mass of the working piece        | 100 Kg         |
| Position lose motion (under cutting) | 0.01mm         |
| Max cutting force                    | 1000 N         |
| Controller design parameters         |                |
| Settling time for velocity loop      | 0.03 Sec       |
| Settling time for position loop      | 0.05 Sec       |
| Robust stability margin              | 1.1            |

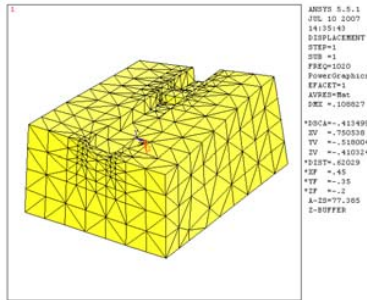
#### A. Mechanical Structure Design

One of the earliest issues that need to be considered in the design process of machine tools is the mechanical structure. The main structure of a feed drive system can be broken into the base, saddle, and table. The structure of a machine tool should be able to support the heavy weight and withstand the cutting action. For this reason, a precision machine has to be carefully designed

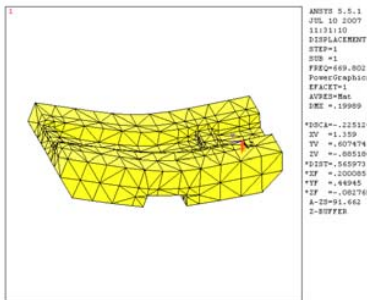
to avoid any undesirable deflection and vibration. Therefore, the stiffness and damping characteristics of structure material for machine tools becomes significant. The most common material used for machine tools is iron because its high damping characteristic is capable of absorbing oscillation and maintaining cutting dynamic stability. However, the density of iron is so high that moving parts are unable to maintain their suitable weights. In addition, processing precision will be easily influenced by thermal deformation due to its high thermal expansion coefficient.

In recent years, in addition to the progress of material science and technology, the use of epoxy granite material (polymer casting) has gradually increased for machine structure [14-15]. It appears that the epoxy granite makes machine's structural element not only lighter (density is 2600 kg/m<sup>3</sup>), but smaller oscillation amplitude than iron. This improvement on material dynamic performance makes the epoxy granite ideal for a high speed machine structural material. Based on the design process described above, the mechanical structure of an experimental feed drive system is designed as shown in Fig. 4, and those structures will be assembled, as shown in Fig. 5. The design objective and constraints can be formulated as (3), where  $I_{N1}$  is the elastic deformation along the Z axis for the feed drive system,  $XX$  and  $XY$  are span distances of X and Y directions for the table, and  $YX$  and  $YY$  are span distances of X and Y direction for the saddle, respectively.

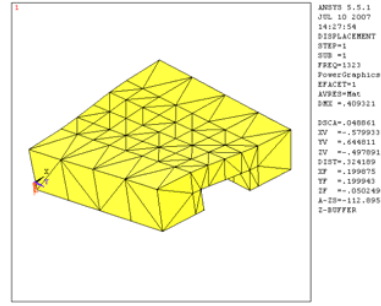
$$\begin{aligned} \min I_{N1} \\ \text{s.t. } 0.072m < XX < 0.328m \\ 0.24m \leq YX \leq 0.65m \\ 0.072m \leq YY \leq 0.328m \\ 0.24m \leq XY \leq 0.31m \end{aligned} \quad (3)$$



(a) Base (mass: 570 Kg, natural frequency: 1020Hz)



(b) Saddle (mass: 140 Kg, natural frequency: 669Hz)



(c) Table (mass: 60 Kg, natural frequency: 1323Hz)

Fig. 4 Main mechanical structures for a feed drive system.

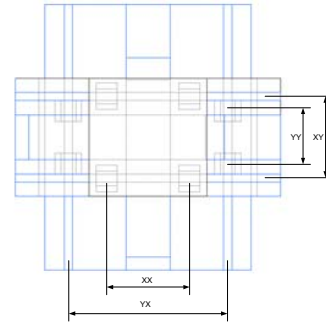


Fig. 5 System assemblies of main mechanical structures for a feed drive system.

### B. Mechanism Components Design

The key point of modeling at the design stage is to obtain a simple model, which is accurate enough to predict the mechanical properties through computer simulation. From section A and Fig. 4, the natural frequencies of each main structures in the feed drive system are much higher than the control bandwidth of design specifications; therefore the free-body diagram of mechanism components for the feed drive system, which includes ball screw, nut, support bearing, linear bearing carriage, coupling, and motor can be modeled as a rigid body and established, as illustrated in Fig. 6 [19]. In this figure, the parameters are defined as below:  $\tau$ : motor torque (N-m),  $F_c$ : cutting force (N),  $J_m$ : rotor inertia (Kg-m<sup>2</sup>),  $J_s$ : ball screw inertia (Kg-m<sup>2</sup>),  $J$ : total inertia  $J_m + J_s$ ,  $M_t$ : table mass (Kg),  $\theta_m$ : motor shaft angle (rad),  $X_t$ : table position (m),  $K_{all}$ : overall stiffness of the feed drive system (N/m),  $C_t$ : damping coefficient of the guide way (N-s/m),  $p$ : lead of ball screw (m), and  $R$ : transformation ratio  $p/2\pi$  (m/rad)

Fig. 3 shows a typical feed drive system. The ball screw is coupled to a rotary servomotor that turns the screw in the bearings. The table and nut are driven via the helical thread of the screw. As a result, in the mechanism components design process, the nut and support bearing are dependent on the ball screw diameter. Consequently, considering the ball screw diameter is the same as considering the system stiffness.

Moreover, the condition of the diameter for the ball screw can be determined by the critical speed; buckling load, and the DN value (see the Appendix for detailed description). On the other hand, in a high-speed machine design, static rigidity and dynamic stiffness are two of the most important characteristics. Based on the above analysis, in this strategy, the objective of the mechanical design parameters  $I_{N2}$  for a feed drive system will aim to obtain maximum stiffness, written as below, where  $10^{-5}$  m and  $d$  are the design target (see the table 1) and the diameter of the ball screw, respectively.

$$\min I_{N2} = (10^{-5} - \frac{F_c}{K_{all}})^2 \quad (4)$$

$$s.t. \quad 8 \times 10^{-3} m < d < 35 \times 10^{-3} m$$

where  $K_{all}$  can be formulated as below, and  $K_s$ ,  $K_b$ , and  $K_n$  are longitudinal stiffnesses of the ball screw, support bearing, nut (N/m), respectively.

$$(1/K_s + 1/K_b + 1/K_n)^{-1} \quad (5)$$

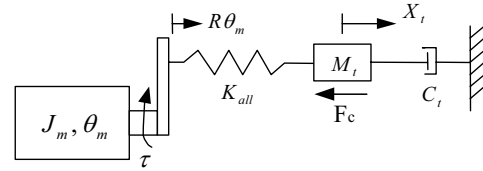


Fig. 6 Free-body diagram of the feed drive system.

TABLE II DESIGN RESULTS

| Mechanical parameters            | DTC Method    |               | ID Method     |               | DFC Method    |               | Variation <sup>1</sup> (%)<br>(ID vs. DFC) |        |
|----------------------------------|---------------|---------------|---------------|---------------|---------------|---------------|--|--------|
|                                  | X axis        | Y axis        | X axis        | Y axis        | X axis        | Y axis        | X axis                                     | Y axis |
| $M_t$ (Kg)                       | 160           | 300           | 157           | 269           | 157           | 269           | -  | -      |
| $J_m$ (Kg-m <sup>2</sup> )       | 13e-4         | 13e-4         | 13e-4         | 13e-4         | 13e-4         | 13e-4         | -  | -      |
| $J_s$ (Kg-m <sup>2</sup> )       | 6.4e-4        | 6.4e-4        | 6.4e-4        | 6.4e-4        | 2.1e-4        | 2.1e-4        | -67  | -67    |
| $K_s$ (N/m)                      | 2.81e8        | 2.81e8        | 2.81e8        | 2.81e8        | 3.43e8        | 3.43e8        | +22  | +22    |
| $K_n$ (N/m)                      | 4.27e8        | 4.27e8        | 4.27e8        | 4.27e8        | 2.6e8         | 2.6e8         | -39  | -39    |
| $K_b$ (N/m)                      | 1e9           | 1e9           | 1e9           | 1e9           | 7.5e8         | 7.5e8         | -25  | -25    |
| $R$ (m/rad)                      | 20e-3/2 $\pi$ | 20e-3/2 $\pi$ | 20e-3/2 $\pi$ | 20e-3/2 $\pi$ | 20e-3/2 $\pi$ | 20e-3/2 $\pi$ | -  | -      |
| Supported distance of X axis (m) | 0.275         | 0.54          | 0.275         | 0.54          | 0.275         | 0.54          | -  | -      |
| Supported distance of Y axis (m) | 0.275         | 0.28          | 0.275         | 0.28          | 0.275         | 0.28          | -  | -      |
| Controller parameters            |               |               |               |               |               |               |  |        |
| $K_p$                            | 1.72          | 1.61          | 1.72          | 1.52          | 1.29          | 1             | -25  | -34    |
| $K_i$                            | 370           | 207.65        | 370           | 218.40        | 267           | 160.7         | -27  | -26    |
| $K_{pp}$                         | 65            | 48            | 65            | 57            | 62            | 53            | -4   | -7     |
| Bandwidth (Hz)                   | 15            | 12.1          | 15            | 15.3          | 16.5          | 16.5          | +10  | +7     |
| Max Control Torque (N-m)         | 14.2          | 10.2          | 14.2          | 11.7          | 11.7          | 9             | -17  | -23    |

<sup>1</sup>: (DFC - ID) / ID

### C. Controller Design

The feed drive system being considered is actually a highly uncertain system with varying multi-resonance modes. The control problem in the feed drive system of machine tools is usually solved based on explicitly or implicitly plant models. However, the plant model may not offer a full description of the real plant due to the simplification in the modeling method, time-varying plant model parameters, etc. The difference between the plant model and the real plant is usually defined as the model uncertainty. Moreover, the real plant of the feed drive system always suffers from various external disturbances during operation. It is very important for design of a control system to ensure the desired performance in the presence of model uncertainty and disturbance. This requirement calls for a robust control design method to be applied to the controller design. Among the robust controller approaches, QFT is a well-known and efficient frequency based robust controller design methodology, which maintains system response within

pre-specified tolerances, despite uncertainties and disturbances, via gain-phase and loop-shaping techniques [16-17]. It has been successfully applied to various engineering applications such as flight controls, missile controls, and control of compact disk mechanisms, etc. The basic idea of QFT is to convert design specifications on closed loop responses and plant uncertainties into robust stability and performance bounds on the open loop transmission of the nominal system. In short, the QFT controller design consists of the following steps;

1. For each particular frequency, templates are developed by determining the frequency responses of various plants. (Fig. 7(a))
2. A set of QFT bounds in Nichols chart is then computed based upon the chosen nominal plant and the design specifications, such as robust margin, robust tracking, and disturbance rejection. Taking the worst-case bound at the same frequency point of the intersection of all bounds gives a single QFT bound in the Nichols chart. (Fig. 7(b))
3. Loop-shaping design technique then is applied to obtain the

controller in order that the QFT bounds in the Nichols chart, at all frequencies, are satisfied and the closed loop nominal system is stable. (Fig. 7(c))

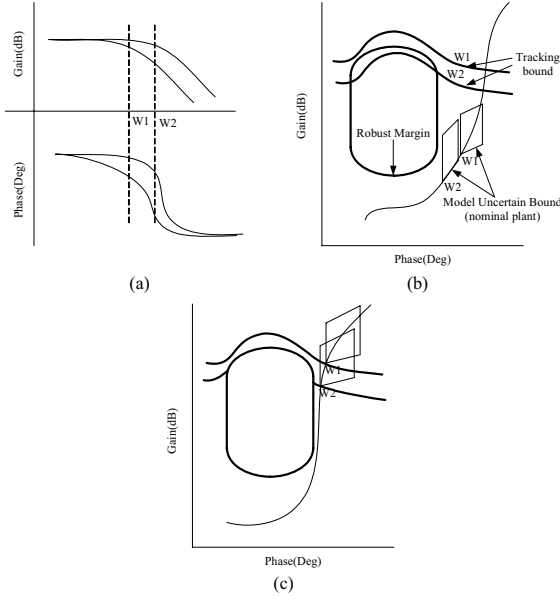


Fig. 7 QFT design procedures.

Before the controller design process, the system dynamic model is illustrated as Fig. 8(a). The corresponding transfer function from the motor torque to motor angle, table velocity, and table position can be respectively calculated as below, where  $\omega_{mech} = \sqrt{K_{all} / M_t}$  and  $\omega_a = \sqrt{K_{all} (1 / M_t + R^2 / J)}$  represent the anti-resonance and resonance frequencies, respectively.

$$\frac{\theta_m}{\tau} = \frac{s^2 + \omega_{mech}^2}{Js^2(s^2 + \omega_a^2)} \quad (6)$$

$$\frac{\dot{X}_t}{\tau} = \frac{\omega_{mech} R}{Js(s^2 + \omega_a^2)} = P_1(s) \quad (7a)$$

$$\frac{X_t}{\tau} = \frac{\omega_{mech} R}{Js^2(s^2 + \omega_a^2)} = P_2(s) \quad (7b)$$

Moreover, in (6), (7a), and (7b), parameters  $K_{all}$  and  $M_t$  are not constant and are functions of the table position and the table load.  $K_{all}$  is varying from  $(1/K_s + 1/K_b + 1/K_n)^{-1}$  to  $(1/K_b + 1/K_n)^{-1}$  according to the position of the table, and  $M_t$  is from 60Kg to 160kg for x axis, and 200kg to 300kg for y-axis based on table load.

Most commercial CNC controllers, such as those servo motion control systems from Fanuc and Siemens in machine tools, cascade controller structures are usually used instead of a single control loop. A simplified cascade controller structure for motion control of a feed drive system is illustrated in Fig. 8(b). In general, it consists of velocity and position control loops, the parameters  $K_{pp}$ ,  $K_p$ ,  $K_i$ ,  $G_1(s)$ , and  $G_2(s)$  are proportional

gain in position loop, proportional gain in position loop, integral gain in velocity loop, transfer function of the velocity controller, and transfer function of the position controller, respectively.

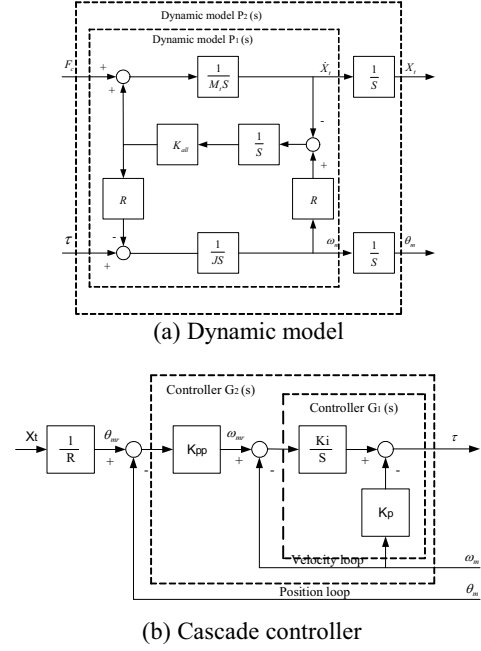


Fig. 8 Dynamic model and cascade controller of a feed drive system.

In QFT, variations in the plant parameters are assumed to occur within known bounds. These variations result in a family of time responses for the plant. Design specifications are selected in order that the time response is satisfactory for the entire family, and time response bounds are used to define frequency response bounds. Therefore, according to Table I, the velocity and position control loop robust design bound can be written as (8) and (9).

$$\left| \frac{P_1(j\omega)G_1(j\omega)}{1 + P_1(j\omega)G_1(j\omega)} \right| \leq 1.1 \quad (8)$$

$$\left| \frac{P_2(j\omega)G_2(j\omega)}{1 + P_2(j\omega)G_2(j\omega)} \right| \leq 1.1 \quad (9)$$

Additionally, the tracking bounds of both loops can be formulated as (10) and (11).

$$T_{VL} \leq \left| F(j\omega) \frac{P_1(j\omega)G_1(j\omega)}{1 + P_1(j\omega)G_1(j\omega)} \right| \leq T_{VU} \quad (10)$$

$$T_{PL} \leq \left| F(j\omega) \frac{P_2(j\omega)G_2(j\omega)}{1 + P_2(j\omega)G_2(j\omega)} \right| \leq T_{PU} \quad (11)$$

where  $T_{VL}$ ,  $T_{VU}$ ,  $T_{PL}$ , and  $T_{PU}$  are velocity loop lower tracking bound, velocity loop upper tracking bound (both corresponding on 0.003 sec settling time for the velocity loop), position loop

lower tracking bound, and position loop upper tracking bound (both corresponding on 0.005 sec settling time for the position loop), respectively. Thus, according to design specifications, the parameters are listed below:

$$T_{VL} = \frac{16129}{0.001(j\omega)^3 + 1.229(j\omega)^2 + 244.7(j\omega) + 16129}$$

$$T_{VU} = \frac{40(j\omega) + 40000}{(j\omega)^2 + 240(j\omega) + 40000}$$

$$T_{PL} = \frac{10404}{0.01(j\omega)^3 + 2.836(j\omega)^2 + 287.6(j\omega) + 10404}$$

$$T_{PU} = \frac{13225}{(j\omega)^2 + 184(j\omega) + 13225}$$

Hence, according to those conditions, the design objective of the controller can be expressed by ITAE (Integrated Time and Absolute Error) criterion and is formulated as (12).

$$I_{R\theta} = \min \int t |e_\theta(t)| dt$$

$$s.t. \quad \tau(t) \leq 14.4$$

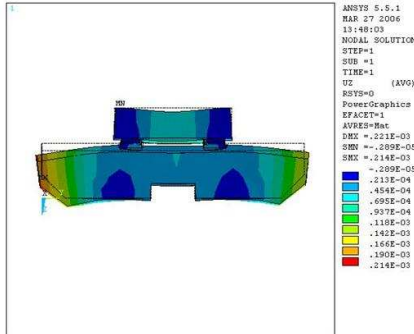
$$e_\theta \geq 0$$
(12)

where:

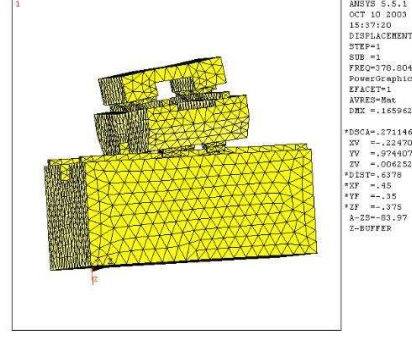
$$e_\theta = \theta_{mr} - \theta_m$$

$$\tau(t) = K_i \int (e_\theta K_{pp} - \omega_m) dt - K_p \omega_m$$

When structure and controller design targets are clear, overall results of feed drive system design parameters can be solved by (3), (4), and (12) and are listed in Table , and the main structure response is shown in Fig. 9.



(a) Static displacement by gravity



(b) First resonance of main structure

Fig. 9 System response of main structure.

#### D. Closed-loop design with ID and DFC Approaches

##### 1) ID approach

To achieve better performance of the feed drive system, either method can be pursued, namely, redesigning the control algorithm or modifying the mechanical structure. The dynamic model, shown in (13), is highly complex and the natural frequency for the feed drive system is determined by three parameters  $K_i$ ,  $\omega_{mech}$  and  $J$ . Therefore, enhancement of the system's performance relies on modification of those three parameters.

$$\frac{\dot{X}_t}{\dot{X}_r} = \frac{K_i \omega_{mech}^2}{Js^2(s^2 + \frac{K_p}{J}s + \omega_a^2) + K_p \omega_{mech}^2 s + K_i(s^2 + \omega_{mech}^2)} \quad (13)$$

According to (13), the control variable  $K_i$  is chosen based on the mechanical characteristic  $\omega_{mech}$ , which has been optimized by the design process. In order to improve the response of the system, a redesign procedure is required. Apparently, improvement of the system's dynamic performance will be determined by  $M_i$  and  $K_{all}$ . Nevertheless,  $K_{all}$  and  $J$  have been obtained as best values by the optimum design process from (4). Accordingly, the optimization process will first focus on the parameter  $M_i$  and seek its better solutions. From the above analysis, mass reduction in the moving table becomes a crucial issue in high-speed machine design. Therefore, according to (13) and (A.7), structural optimization has the ability to reduce the system inertia and increase natural frequency at the same time.

In both  $X$  and  $Y$  axes of the feed drive system, the parameter  $M_i$  represents the overall mass of the moving parts, which includes the work piece, the table, and the saddle. The shapes of the saddle and the table for the first design result are shown in Fig. 4. The mechanical characteristics of the saddle and table can be solved by the approach of the Finite Element Method (FEM). The value of  $M_i$  directly affects the physical properties of the saddle and table. Additionally, the dynamic behavior of a machine tool is mostly dominated by its natural frequency. The response of a structure to low frequency excitations is mainly a



function of the first natural frequency and its mode shapes. In the feed drive system design, frequency requirements can be used to prevent chatters during machining. Consequently, the saddle is therefore modified to be less weight without reducing the structurally natural frequency. Hence, a number of well-known methods, such as sizing, shaping, and topology optimization are considered in this interactive design process to improve structural performance.

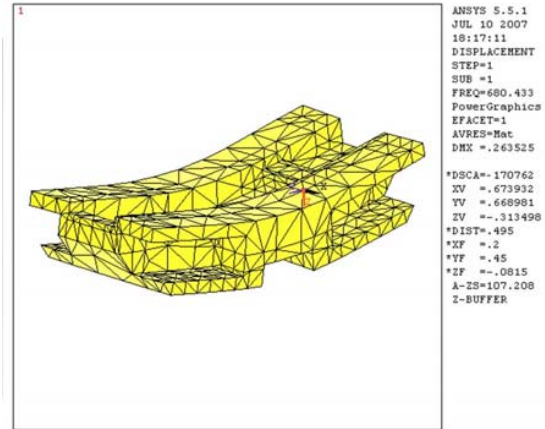
Among those structure optimization methods, the topology optimization has drawn significant attention in recent developments of structural optimization. This method has been proved effective in determining the initial geometric shape for structural designs [19]. However, its major drawbacks are that a non-smooth structural geometry is always resulted and the manufacturing process becomes difficult or non-cost-effective [18]. Based on those restrictions, the shape optimization is chosen to reduce the weight of the main structure.

For the saddle and table shape optimization problem, the Euler-Bernoulli beam equation (14) shows the I-beam is a very efficient form for carrying both bending and shears in the plane, where  $u(x_1)$  describes the deflection  $u$  of the beam at some position  $x_1$ ,  $\omega$  is a distributed load,  $E$  is the elastic modulus and  $I$  is the second moment of area. Additionally, the cross-section has a reduced capacity in the transverse direction. Therefore, in this shape optimization, the I-beam is considered.

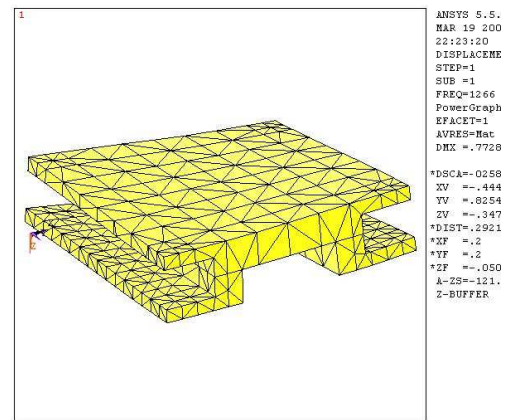
$$\frac{\partial^2}{\partial x_1^2} \left( EI \frac{\partial u}{\partial x_1^2} \right) = \omega \quad (14)$$

Fig. 10 (a) and (b) illustrate that the saddle mass and table mass are decreased by 28 Kg to 112 Kg and by 5 Kg to 55Kg, respectively. Furthermore, the first resonant frequency of the saddle rises to 680 Hz, from 669 Hz. Nevertheless, the 1<sup>st</sup> nature frequency for the table reduces to 1266 Hz as shown in Fig. 10(b). The main reason is that I-beam is inefficient in the torsion mode (Fig. 4(c)). As a result, the shape of the saddle is modified to be 57 kg with the 1<sup>st</sup> nature frequency at 1329 Hz as depicted in Fig. 10(c).

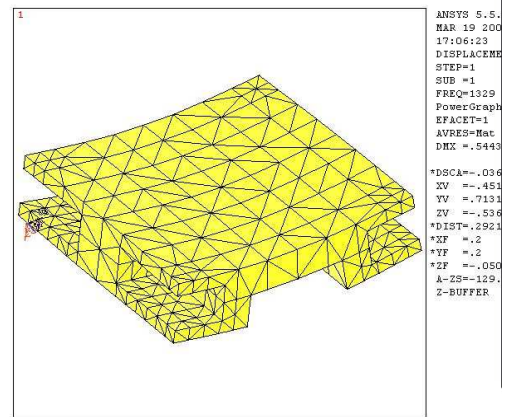
After the saddle and table for the feed drive system are modified, a set of new controller parameters are obtained by employing (9), (10), (11), and (12). The final design parameters are also listed in Table II. The bandwidth of the position loop for X and Y axes are increased from 15Hz to 15.5 Hz and 12.5 Hz up to 15.3 Hz, respectively.



(a) Shape optimization for the saddle



(b) Mass reduction using I-beam for the table



(c) Shape optimization for the table

Fig. 10 Dynamic performance of the new design for the saddle and the table.

## 2) DFC approach

Based on the iterative design methodology described in previous section, both mechanical and control parameters are considered as design variables. In this study,  $M_i$ ,  $J_m$ ,  $J_s$ ,  $K_s$ ,



$K_n$ ,  $K_b$ ,  $R$ , as well as controller gains,  $K_{pp}$ ,  $K_p$ ,  $K_i$  of the position loop and the velocity loop are respectively selected as design variables  $X_N$  and  $X_R$ . As results show in Table II, when the performance is improved, the maximum control torque is increased as well. On the other hand, during the iterative design process, the results for (4) are still fixed. Therefore, this strategy only re-considers the system mass during this process. Thus, in order to achieve the optimization solution for the system level, simultaneous design strategy must be conducted.

For the DFC approach, a new system-level objective function is formulated as (15), where  $I$  is the objective of the system-level for the feed drive system, and  $\alpha$ ,  $\beta$ ,  $\gamma$ , and  $\sigma$  are weighting factors. In view of the different engineering units and system level requirements, 100, 100, 5, and 1, are selected, respectively.

$$I = \min(\alpha I_{N1} + \beta I_{N2} + \gamma I_{R\theta} + \sigma \tau(t)) \quad (15)$$

Consequently, according to this objective function, the overall results for system design parameters are listed in Table II, the control cost is reduced 17% for  $X$  axis and 23% for  $Y$  axis, via the DFC approach. Thus, the control cost is smaller than DTC and ID, and system performance is higher than those strategies (16.5 Hz for DFC strategy, 15 Hz for ID strategy). The main reason for these results is that  $K_{all}$  and  $J$  are considered and balanced simultaneously during the design process. In addition, the open loop control characteristic curve form QFT loop shaping, both time and frequency domain response, of  $X$  and  $Y$  axes are shown in Fig. 11 and Fig. 12, respectively.

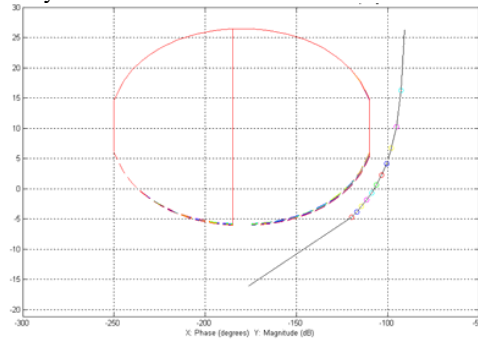
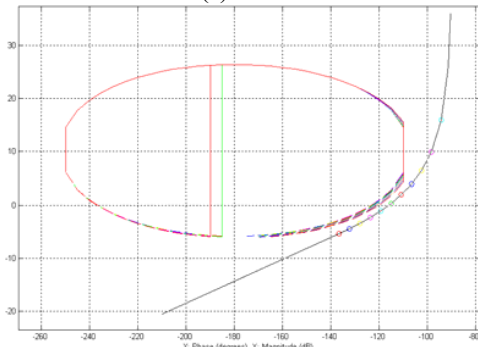
(a)  $X$  axis(b)  $Y$  axis

Fig. 11 Loop shaping from QFT.

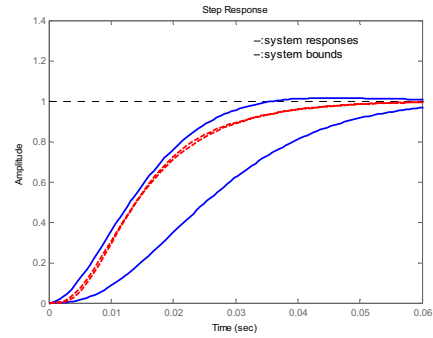
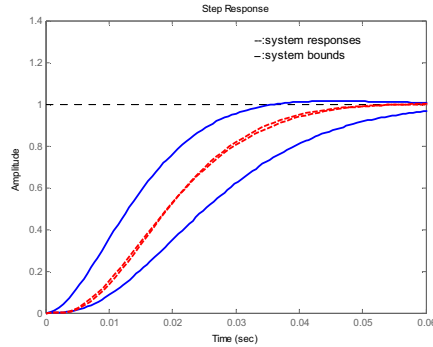
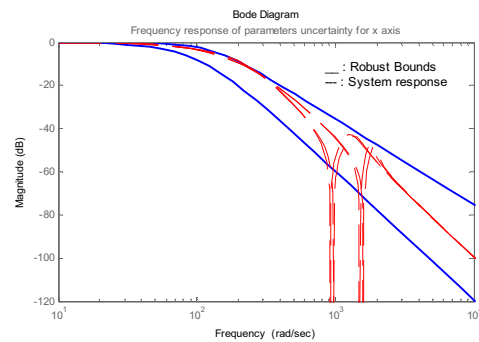
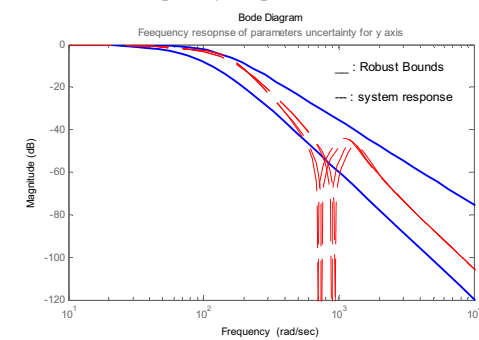
(a) Time domain response of  $X$  axis(b) Time domain response of  $Y$  axis(c) Frequency responses of  $X$  axis(d) Frequency responses of  $Y$  axis

Fig. 12 System responses of the position loop.

From the above analysis, Fig. 13 demonstrates comparison among those three design strategies in terms of system performance and control cost. Both sequential and iterative

approaches just consider system performance; as a result, the corresponding control cost increases simultaneously. Conversely, for the DFC method, the design parameters of structure and control design are improved simultaneously; and therefore, in addition to the system performance, control cost is also reduced during the iterative design process.

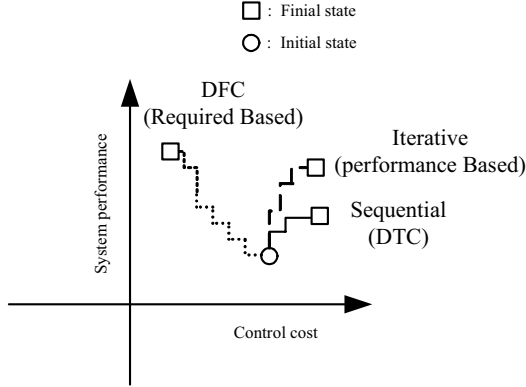


Fig. 13 Control cost in iterative process.

#### IV. CONCLUSIONS

The model-based robust integrated design technology of a mechatronic feed drive system for machine tools is proposed in this paper. Both structural dynamics and control are optimized during the integrated design processes, through 3D model analysis and the QFT approach, via the DFC method. In addition, during structural and control iterative design processes, the DFC method is employed simultaneously, to improve structural characteristics and control performance. The proposed design scheme improves the quality of the design processes and makes it possible to reduce the amount of experimentation required to deliver an optimized hardware prototype into operation.

The focus of this paper is only at performance for basic control loops in the feed drive system of machine tools. To achieve completely robust integrated design of a feed drive system for machine tools, contour errors will be considered for the future research work.

#### V. APPENDIX

Formulations of main design parameters are listed as below:

Lead for screw:

$$p \geq V_{\max} / N_m \quad (\text{A.1})$$

where

$p$  : Lead for screw (m)

$V_{\max}$  : Maximum motion speed (m/min)

$N_m$  : Maximum speed for motor (rpm)

Buckling load:

$$p_b = \frac{n \times \pi^3 \times E \times d^4}{64L^2} \quad (\text{A.2})$$

where

$p_b$  : Buckling load (N)

$n$  : Weighting factor,  $n = 2.0$  for the fix-support structure

$E$  : Elastic modulus of screw = 207 Gpa

$d$  : Screw diameter (m)

$L$  : Span of the screw shaft (m)

$$N_c = \frac{60\lambda^2}{2\pi L^2} \sqrt{\frac{EIg}{\gamma A}} \quad (\text{A.3})$$

Critical speed:

$$N_c = \lambda \frac{d}{L^2} \times 10^{10} \quad (\text{A.4})$$

where

$N_c$  : Critical speed (rpm)

$\lambda$  : Weighting factor for setting type,  $\lambda = 15.1$  (fix-support)

DN value:

$$d \cdot N_{\max} < 70000000 \quad (\text{A.4})$$

where

$N_{\max}$  : Maximum speed for screw shaft (rpm)

Longitudinal stiffness of screw:

$$K_s = \frac{\pi d^2 E}{4L} \quad (\text{A.5})$$

Rotor inertia of screw:

$$J_s = \frac{\pi \rho L d^4}{32} \quad (\text{A.6})$$

where

$\rho$  : Density of the screw shaft (kg/m)

Equivalent rotor inertia of table

$$J_t = W \left( \frac{p}{2\pi} \right)^2 \quad (\text{A.7})$$

where

$W$  : Overall mass (Table mass + work piece mass) (kg)

#### REFERENCES

- [1] A.L. Hale, R.J. Lisowski, and W.E. Dahl, "Optimal simultaneous structural and control design of maneuvering flexible spacecraft," *J. of Guidance, Control, and Dynamics*, Vol. 8, No.1, pp. 86-93, 1985.
- [2] D.S. Bodden, and J.L. Junkins, "Eigenvalue optimization algorithms for structure/controller design Iterations," *J. of Guidance, Control, and Dynamics*, Vol. 8, No. 6, pp. 697-706, 1985.
- [3] A. Messac, "Control-structure integrated design with closed-form design metrics using Physical Programming," *AIAA J.*, Vol. 36, No. 5, pp. 855-864, 1998
- [4] J.H. Park, and H. Asada, "Concurrent design optimization of mechanical structure and control for high speed robots," *ASME J. of Dyn. Syst. Meas. and Control*, Vol. 116, pp. 344-356, Sep., 1994.
- [5] A.C. Pil, and H. Asada, "Integrated structure/control design of mechatronic system using a recursive experimental optimization method," *IEEE/ASME Trans. on Mechatronics*, Vol. 1, No. 3, pp.191-203, 1996.
- [6] Y.P. Yang, and C.C. Tu, "Multiobjective optimization of hard disk suspension assemblies: Part I-Structure design And sensitivity analysis," *Computer & Structures*, 757-770, 1996.
- [7] Y.P. Yang, and C.C. Tu, "Multiobjective optimization of hard disk suspension assemblies: Part II-Integrated structure and control design," *Computer & Structures*, Vol. 59, No. 4, pp. 757-770, 1996.

- [8] K. Fu, and J. K. Mills, "A convex approach solving simultaneous mechanical structure and control system design problems with multiple closed-loop performance specifications," *ASME J. Dyn. Syst. Meas. and Control*, Vol. 127, pp. 57-68, 2005.
- [9] G. Reinhart, and M. Weissenberger, "Multibody simulation of machine tools as mechatronic systems for optimization of motion dynamics in the design process," In Proceedings IEEE/ASME International Conference on *Advanced Intelligent Mechatronics*, pp. 605-610, 1999
- [10] J. V. Amerongen, and P. Breedveld, "Modelling of physical systems for the design and control of mechatronic systems," *Ann. Reviews in control*, Vol. 27, No. 1, pp. 87-117, 2003.
- [11] Gianni Ferretti, GianAntonio Magnani and Paolo Rocco, "Virtual prototyping of mechatronic systems," *Ann. Reviews in Control*, Vol. 28, No. 2, pp. 193-206, 2004
- [12] A. Chattopadhyay, and N. Pagalapati, "A multidisciplinary optimization using semi-analytical sensitivity analysis procedure and multilevel decomposition," *Computers & Mathematics with Applications*, Vol. 29, No. 7, pp. 55-66, 1995.
- [13] Q. Li, W.J. Zhang, and L. Chen, "Design for control-a concurrent engineering approach for mechatronic system design" *IEEE/ASME Trans. on Mechatronics*, Vol. 6, No. 2, pp. 161-169, 2001.
- [14] S Jung, C. J., Lee, E. and S. H. Cheng, "Design of inspecting machine for next generation LCD glass panel with high modulus carbon/epoxy composites," *Composite Structures*, Vol. 66, pp. 439-447, 2004.
- [15] X. Luo, K. Cheng, D. Webb, and F. Wardle, "Design of ultraprecision machine tools with applications to manufacture of miniature and micro components," *J. of Materials Processing Technology*, Vol. 167, No. 2-3, pp. 515-528, 2005.
- [16] I. Horowitz, "Survey of Quantitative Feedback Theory," *Int. J. Control*, Vol. 53, No. 2, pp. 255-291, 1991.
- [17] A.C. Zolotas, and G.D. Halikias, "Optimal design of PID controllers using the QFT method," *IEE Proc.-Control Theory and Applications*, Vol. 146, No. 6, pp. 585-589, 1999.
- [18] W. Nadir, I. Y. Kim, and O. L. de Weck, "Structural Shape Optimization Considering Both Performance and Manufacturing Cost," In *Proceedings 10th AIAA/ISSMO Multidisciplinary Analysis and Optimization Conference*, 2004
- [19] J.-S. Chen, Y.-K. Huang, and C.-C. Cheng, "Mechanical model and contouring analysis of high-speed ball-screw drive systems with compliance effect," *The International Journal of Advanced Manufacturing Technology*, Vol. 24, No.3-4, pp. 241-250, 2004.
- [20] M. Ebrahimi, and R. Whalley, "Analysis, modeling and simulation of stiffness in machine tool drives," *Computers and Industrial Engineering*, Vol. 38, No. 1, pp. 93-105, 2000.

**Chin-Yin Chen** was born in Taoyuan, Taiwan, R.O.C., in 1976. He received the degree in mechanical engineering and the master degree from the Da-Yeh Univ. in 1998 and 2000, respectively. He is currently a Ph.D. student with the Department of Mechanical and Electro-Mechanical Engineering of the National Sun Yat-Sen University, Kaohsiung, Taiwan, R.O.C.

His research interests include mechatronics, integrated structure/control design, and robotics.

**Chi-Cheng Cheng** was born in Taipei, Taiwan, R.O.C., in 1959. He received the B.S. degree and the M.S. degree in power mechanical engineering from National Tsing Hua University, Hsinchu, Taiwan, in 1981 and 1983, respectively, and the Sc.D. in mechanical engineering from Massachusetts Institute of Technology, Massachusetts, in 1991. He is currently a Professor with the Department of Mechanical and Electro-Mechanical Engineering, and a Adjoin Professor with the Institute of Applied Marine Physics and Undersea Technology of the National Sun Yat-Sen University, Kaohsiung, Taiwan, R.O.C. His research interests are in the areas of system dynamics and control, machine vision, fuzzy modeling and control, and telerobotics.